Front. Optoelectron. 2014, 7(3): 385–392
DOI 10.1007/s12200-014-0421-7

RESEARCH ARTICLE

Absorption density control in waveguide photodiode–analysis, design, and demonstration

Dingbo CHEN (✉), Jeffery BLOCH, Rui WANG, Paul K. L. YU

Department of Electrical and Computer Engineering, University of California, San Diego, 9500 Gilman Dr, La Jolla, CA 92093, USA

Abstract A modal analysis is conducted for analyzing the absorption profile of high power waveguide photodiodes designed for analog optical link. The excitation of guided modes with large filling factor in the absorber is identified as a limiting factor for the performance of waveguide photodiodes at high optical power, including power handling capability, and bandwidth-efficiency product. A waveguide photodiode design, which spatially separates the input waveguide from the absorber in the lateral direction, is analyzed and experimentally demonstrated to suppress the excitation of mode with large filling factor. Photocurrent > 60 mA under -4 V bias is measured, with 0.80 A/W responsivity. This design illustrates that high power handling capability can be achieved without compromising the bandwidth-efficiency product.

Keywords photodiode, waveguide, thermal failure, high power, mode excitation

1 Introduction

Analog fiber optical link is widely used for distribution of cable TV signal, and in conveying the signals to and from antennas. As optical-to-electrical converter in the analog fiber optical link, photodiodes with high absorption efficiency over wide frequency range at high optical power level are desirable for satisfying the requirements of high dynamic range and high bandwidth [1]. Two types of photodiode (PD) structures have been investigated, namely, the surface normal (SN) and the waveguide (WG) photodiodes. In SNPD, the radiation is absorbed as it is incident normally to the absorption layer and propagates through the detector structure. The photo-generated carriers have to travel through approximately the optical radiation absorption path. The thicker the absorption layer, the higher is the efficiency, and the longer is the carrier transit time [2]. This limits the highest bandwidth-efficiency product achievable in SNPD designed for high power applications, whose surface area size can typically be so large that the device resistance-capacitance (RC) time constant and carrier transit time become comparable. In WGPD, a detector structure containing an absorber locates within or next to a waveguide. While the optical radiation propagates along the waveguide and gradually get absorbed, the photo-generated carriers travel through the detector structure in a direction transverse to the waveguide. Therefore, in WGPD the carrier transit time is not affected by the optical absorption path, which allows the reduction of transit time by using thinner absorber, while maintaining high efficiency by using sufficiently long longitudinal absorption path, and results in bandwidth-efficiency products that can exceed that of SNPD devices [3].

For high power operations at 1.55 μm wavelength, various traditional waveguide integrated photodiode (WIP) designs have been reported [4–8], which usually include a passive section and an active section. A schematic of this type of WIP is shown in Fig. 1. In the passive section, an input waveguide stabilizes the incident optical radiation in certain modes (mostly the 0^{th} order mode), which then excite various modes in the active section, with an absorber on top of the waveguide. At the front end of the active section, the absorption density is close to zero, as the optical power is confined in the waveguide and little is in the absorber. The absorption profile in the whole active section depends on the WIP design. Generally, this type of traditional WIP design has a bandwidth-efficiency product greater than that of SNPD, as discussed previously. However, when designed for high power applications, a trade-off between the absorption efficiency and bandwidth in the traditional WIP designs appeared [8,9]. This is because the confinement factor in the absorber, which represents the power portion in a WIP that is confined in the absorber, is usually designed to be small for high power

Received February 18, 2014; accepted March 12, 2014

E-mail: dic002@ucsd.edu

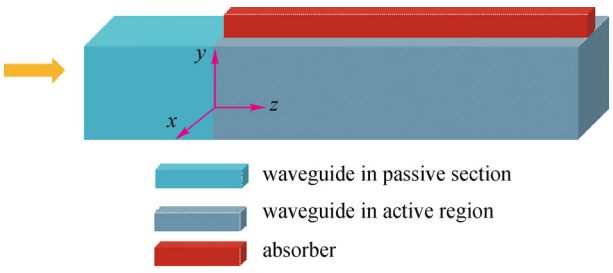

Fig. 1 Schematic of traditional WIP for high power applications

detection, thus requires longer absorber length to achieve high absorption efficiency, and reduces the RC time limited bandwidth.

In this paper, a modal analysis of the traditional WIP design is presented, with factors limiting the bandwidth-efficiency product at high power identified. A novel waveguide photodiode design previously proposed by our group [10] is analyzed here using similar modal analysis. We theoretically and experimentally show that this waveguide design can perform very well even under high power, without the limitation of the trade-off between bandwidth and absorption efficiency that exists in traditional high power WIP designs.

2 Analysis of WIP's high absorption near the front end

In traditional WIP designs, the absorption near the front end limits the high power performances [8,10,11]. A thermally failed traditional WIP fabricated in our group is shown in Fig. 2, in which the high absorption near the front end results in localized thermal damage near the beginning of the active section. The high absorption near the front end in traditional WIP relates to a common feature of modes excitation at the active section. A cross-section view of a traditional WIP structure is shown in Fig. 3(a) for our discussion. As noted earlier, the passive input waveguide couples the incident optical radiation into its 0^{th} mode, which then excites various modes in the active section. Among all the excited modes, the 0^{th} and 1^{st} order modes, $\Phi_0(x,y)$ and $\Phi_1(x,y)$, are of interest. These two modes are simulated by FIMMWAVE[1]. As shown in Fig. 3(b), in the x direction, the two modes have large overlap with the input mode, and therefore they can be significantly excited. However, in the y direction, $\Phi_0(x,y)$ is more confined in the waveguide, whereas $\Phi_1(x,y)$ is more confined in the absorber. In this case, the Γ of $\Phi_1(x,y)$, which is the filling factor in the absorber and is defined as the power portion distributed in the absorber in a

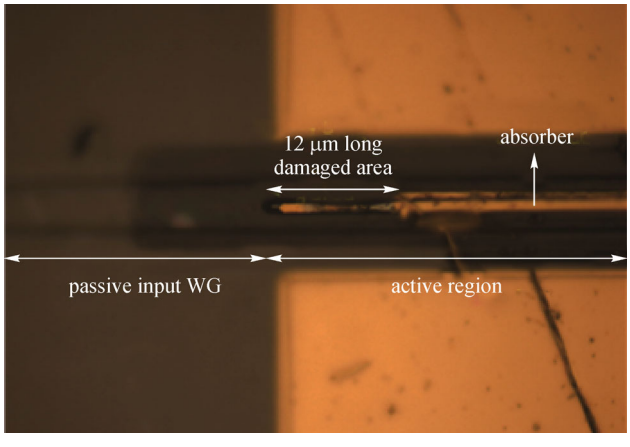

Fig. 2 Top view of thermally failed WIP with traditional WIP structure

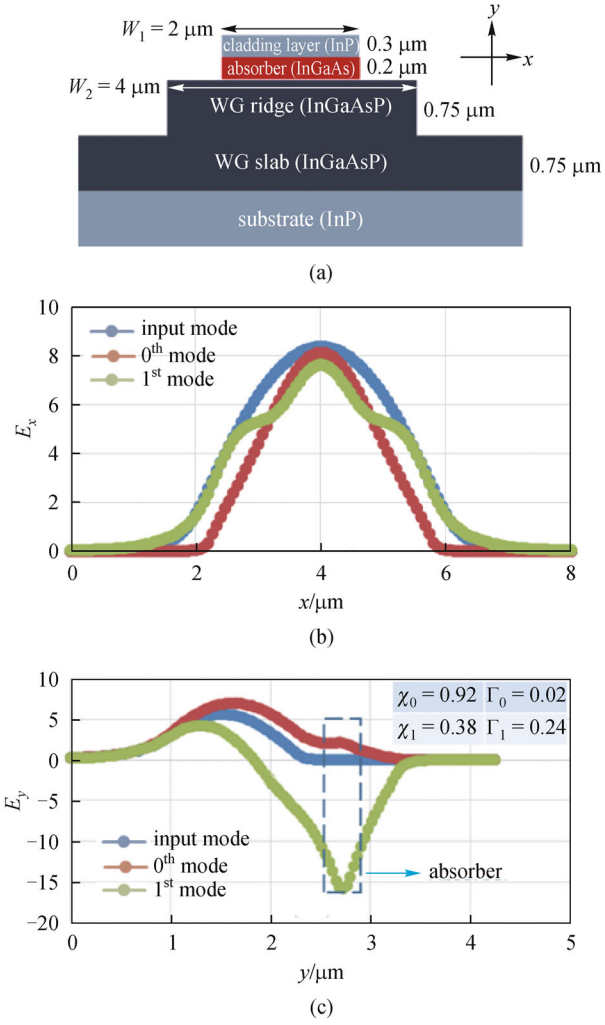

Fig. 3 Cross-sectional view of example of traditional WIP (a); field plot for the 0^{th} and 1^{st} order modes at the center of waveguide along x direction (b) and y direction (c)

1) FIMMWAVE is a suite of robust and fully vectorial mode solvers for 2D + Z waveguide structures, which is developed by Photon Design Inc.

mode, is much larger than that of $\Phi_0(x,y)$.

With the 0th and 1st order modes being excited significantly, for the simplicity of discussion, assuming other higher order modes only account for very small portion of the total power, the total field in WIP active section can be written as the weighted sum of $\Phi_0(x,y)$ and $\Phi_1(x,y)$.

$$\Phi(x,y,z) \approx \chi_0\Phi_0(x,y)\mathrm{e}^{-\beta_0 z} + \chi_1\Phi_1(x,y)\mathrm{e}^{-\beta_1 z}, \quad (1)$$

where χ_0 and χ_1 are the excitation coefficients of the 0th and 1st order modes, β_0 and β_1 are the propagation constant of the 0th and 1st order modes. As mentioned before, the optical power at the absorber front end ($z = 0$) is close to zero. For a WIP structure with given $\Phi_0(x,y)$ and $\Phi_1(x,y)$, this boundary condition determines the excitation coefficients χ_0 and χ_1, as shown in Eq. (2). The more comparable the power distributed in absorber in the 0th and 1st order modes is, the closer χ_0 and χ_1 are.

$$\begin{aligned}&\Phi_{\text{active region}}(x,y)|_{\text{absorber},z=0^+}\\ &= |\chi_0|\Phi_0(x,y)|_{\text{absorber},z=0^+}\\ &\quad + |\chi_1|\Phi_1(x,y)|_{\text{absorber},z=0^+}\\ &= \Phi_{\text{input}}(x,y)|_{\text{absorber},z=0^-} \approx 0.\end{aligned} \quad (2)$$

The mode excitation condition in all traditional WIPs is more or less similar due to the above boundary condition. More complicated WIP structure, for example with larger dimensions and more layers, may add more details to the modes' field profile, or generate more higher order modes. However, both the 0th and 1st order modes would always be excited significantly by the 0th mode of the input waveguide in the passive section, due to their large mode overlap.

The 0th and 1st order modes beat with each other as they propagate forward in the WIP, the power in the absorber is proportional to the integrated intensity.

$$\begin{aligned}&P_{\text{absorber}}(z)\\ &\propto \iint_{\text{absorber}} \Phi\Phi^* \mathrm{d}x\mathrm{d}y\\ &= \chi_0^2\mathrm{e}^{-\alpha_0 z}\iint_{\text{absorber}} \Phi_0\Phi_0^* \mathrm{d}x\mathrm{d}y\\ &\quad + \chi_1^2\mathrm{e}^{-\alpha_1 z}\iint_{\text{absorber}} \Phi_1\Phi_1^* \mathrm{d}x\mathrm{d}y\\ &\quad + 2\chi_0\chi_1\cos\Big(\mathrm{Re}(\beta_0-\beta_1)z\Big)\mathrm{e}^{-(\alpha_0+\alpha_1)z/2}\\ &\quad \iint_{\text{absorber}} \Phi_0(x,y)\Phi_1^*(x,y)\mathrm{d}x\mathrm{d}y\\ &= \chi_0^2\Gamma_0\mathrm{e}^{-\alpha_0 z} + \chi_1^2\Gamma_1\mathrm{e}^{-\alpha_1 z}\\ &\quad + 2\chi_0\chi_1\cos\Big(\mathrm{Re}(\beta_0-\beta_1)z\Big)\mathrm{e}^{-(\alpha_0+\alpha_1)z/2}\\ &\quad \iint_{\text{absorber}} \Phi_0(x,y)\Phi_1^*(x,y)\mathrm{d}x\mathrm{d}y,\end{aligned} \quad (3)$$

where Γ_0 and Γ_1 are the confinement factor in the absorber of the 0th and 1st order modes. Noting that $\Phi_0(x,y)$ and $\Phi_1(x,y)$ have opposite sign at the absorber (as shown in Fig. 3(c)), so Eq. (3) can be re-written as

$$\begin{aligned}&P_{\text{absorber}}(z)\\ &\approx \chi_0^2\Gamma_0\mathrm{e}^{-\alpha_0 z} + \chi_1^2\Gamma_1\mathrm{e}^{-\alpha_1 z}\\ &\quad - 2\chi_0\chi_1\cos\left(\frac{2\pi}{\lambda}\mathrm{Re}(n_{\text{eff},0}-n_{\text{eff},1})z\right)\\ &\quad \times\left|\iint_{\text{absorber}} \Phi_0(x,y)\Phi_1^*(x,y)\mathrm{d}x\mathrm{d}y\right|\mathrm{e}^{-(\alpha_0+\alpha_1)z/2}.\end{aligned} \quad (4)$$

In Eq. (4), the power in propagation in the absorber is the sum of power represented in three terms. The first two terms represent the power in 0th and 1st order modes in the absence of beating, whereas the third term represents the power in beating between the two modes. All three terms carry an exponential attenuation function in the form of $\exp(-\alpha z)$. This exponential function in each term represents the attenuation of power due to absorption, so $1/\alpha$ is the absorption length. As α is large for mode with large Γ [1], α_1 is usually much larger than α_0, which is also shown in Fig. 3. The absorption near the front end is closely related to the last two terms, since their exponential functions carry α_1 and thus small absorption length. The power in those two terms gets absorbed within short propagation distance from front end, and contributes to the high absorption there. In this regard, the absorption near the front end is closely related to the 1st order mode with large α_1 and Γ. The excitation coefficient of 1st order mode χ_1 determines the magnitude of absorption peak near the front end, as shown in Fig. 4. Larger χ_1 corresponds to a higher absorption peak near the front end. In the cases shown in Fig. 4, it corresponds to peak position 10 μm away from the absorber front end, which is in good agreement with the observed failed WIP shown in Fig. 2.

3 Directional coupler photodiode (DCPD) for better absorption front end absorption control

As discussed, the relatively high excitation of the 1st order mode with large Γ and hence large absorption near the front end in traditional WIP is caused by the large mode overlap between input mode and large Γ mode in the x direction. By spatially separating the two modes, we can reduce the excitation of large Γ mode and suppress the

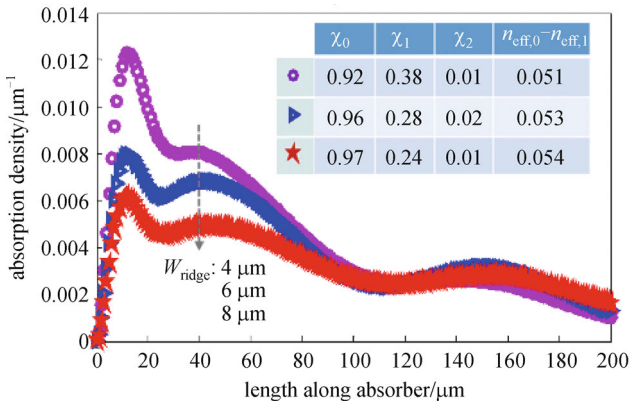

Fig. 4 Simulated absorption profile in traditional WIP shown in Fig. 3(a), with WG ridge width, W_2 varied. The mode excitation coefficient χ of first three major modes 0^{th}, 1^{st}, and 2^{nd} are listed in an enclosed table, while all other modes with $\chi < 0.01$ are neglected.

absorption near the front end. Figure 5 shows a comparison of WIPs with different spatial x-separation (δx) between input waveguide and absorber. It can be observed that larger δx corresponds to a lower absorption near the front end, as well as a larger separation between the absorption peak location and the absorber front end. The resultant DCPD design was first reported in Ref. [10], with the special feature that the input waveguide and absorber are spatially separated in the x direction. As shown in Fig. 6, it also includes an input transitional waveguide, which transfers the incident optical radiation and excites multiple modes in the multimode interference (MMI). An absorber structure, which laterally separates from the input waveguide, locates on top of the MMI. A passive propagation section of the MMI with certain length, denoted as the delay length, is added to control the optical power that is coupled from input waveguide to the frontal section of absorber. The longer the delay length is, the more optical power is incident at the absorber front end. The width of optical waveguide is tapered later on to enhance power density in MMI and improve the absorption efficiency.

The mode excitation mechanism in DCPD is quite different from that in the traditional WIP, as a result of the spatial separation between absorber and input waveguide. In traditional WIP, the large Γ mode (the 1^{st} order mode) is excited directly by the input mode. Large mode overlap between the two results in great excitation of the large Γ mode. However, in DCPD, the input mode first excites multiple modes in the MMI, which then propagate along

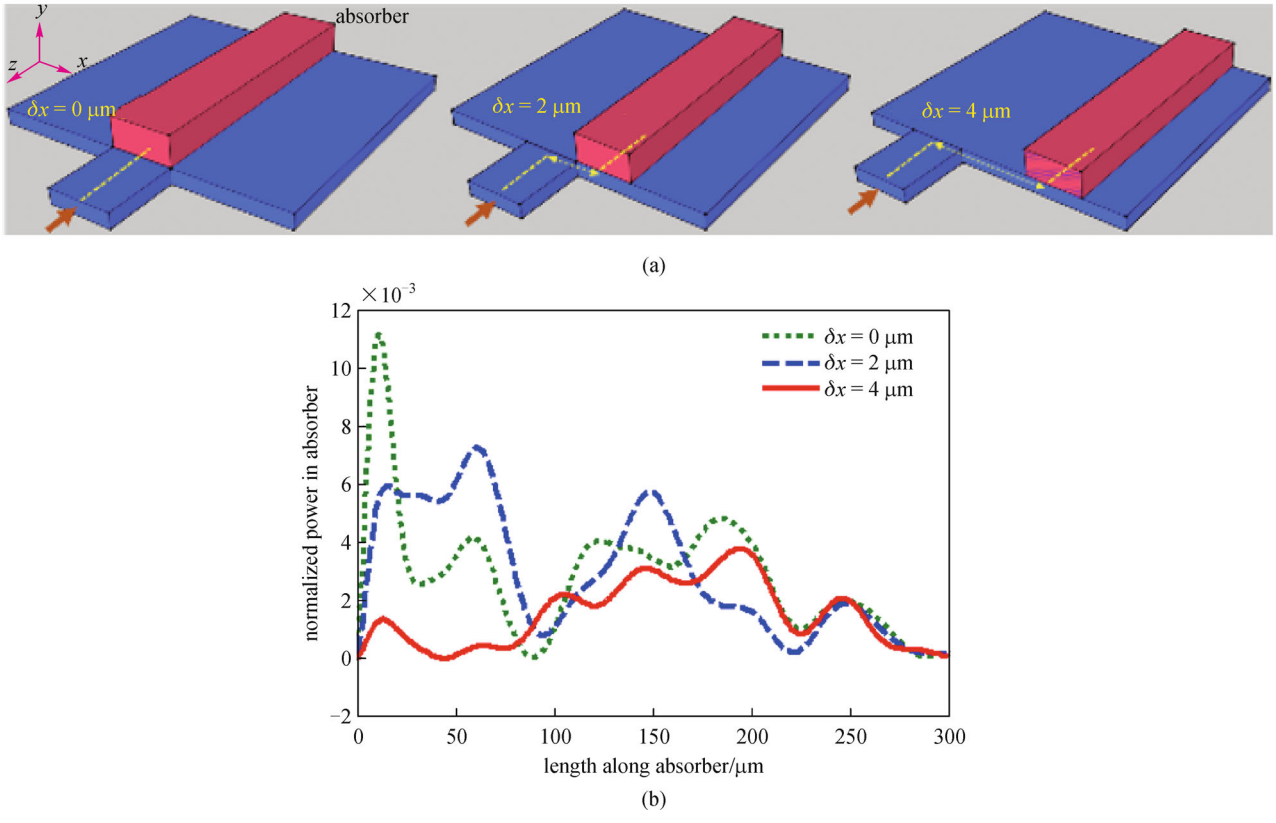

Fig. 5 Comparisons of waveguide structure (a) and absorption profile (b) among WIPs with different spatial separation δx between input waveguide and absorber at x direction

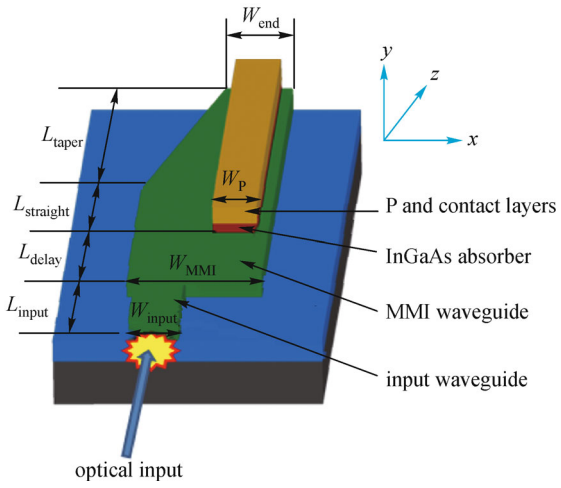

Fig. 6 Schematic of DCPD

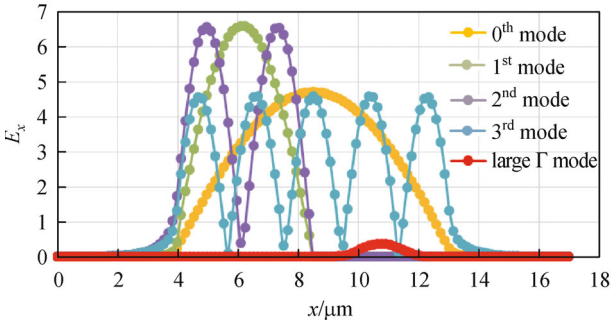

Fig. 7 Field plot for first 4 major modes in the passive MMI and large Γ modes in DCPD active section along *x* direction

Table 1 Excitation coefficient χ and filling factor Γ of the first 5 major modes and the large Γ mode in DCPD

mode	excitation coefficient χ	filling factor Γ
0^{th}	0.34	0.010
1^{st}	0.51	0.011
2^{nd}	0.43	0.050
3^{rd}	0.15	0.040
4^{th}	0.11	0.080
5^{th}	0.03	0.070
large Γ mode	0.002	0.240

the delay length and excite a new set of modes at the active section. As shown in Fig. 7, the 0^{th}, 1^{st}, 2^{nd}, and 3^{rd} models are the first four major modes excited in MMI by the input waveguide. As they have very small overlap with the large Γ mode in DCPD, the excitation of large Γ mode can be suppressed. Moreover, the modes excited in DCPD have Γ difference much smaller than in traditional WIP, as shown in Table 1. Large absorption near front end can thus be avoided in DCPD through the combined design of the spatial separation and the delay length of the MMI.

The DCPD was proposed in our group previously, with some preliminary measurement results reported for some design parameters [10]. In this paper, the DCPD layer structure and waveguide structure are optimized. The epi-layer structure, waveguide structure, as well as the Beamprop simulated absorption profile is shown in Fig. 8. The 2 μm × 200 μm absorber mesa sits on top of a 9 μm wide MMI, with 4.5 μm center-to-center separation from input waveguide at *x* direction, and 90 μm from the front end of MMI. The layer structure includes a modified uni-traveling-carrier (MUTC) structure [10] for high power and speed considerations, with 0.2 μm thick InGaAs absorber and 0.4 μm thick intrinsic InGaAsP layer. The simulated DCPD absorption profile has absorption peak-to-average ratio of 1.5 and responsivity of 0.85. When compared to reported simulated results in the traditional WIP [8,11], DCPD achieves more uniform absorption distribution.

DCPDs with various delay lengths are fabricated on an epi-wafer with MUTC structure, as shown in Fig. 8. Traditional WIP devices are also fabricated on the same wafer. Compare to DCPD, they have the same waveguide and absorber width at the beginning of the active section. The epitaxial layers are grown by Molecular-Beam-Epitaxy on a Fe-doped semi-insulating InP substrate. Fabrication of DCPD is done using photo-lithography and wet etching. The wafer is lapped down to ~100 μm thick and is cleaved into arrays, and then is mounted on copper mount with thermal conductive Epoxy. The optical test of DCPD is performed in an environment with low moisture and at constant temperature. Devices are aligned with lensed SMF fiber. DCPD with various delay length, as well as traditional WIP, are tested at around 1.55 μm wavelength and −4 V dc bias voltage, as shown in Fig. 9. Even though they exhibit similar responsivity, DCPDs with shorter delay length is able to handle higher optical power. Photocurrent > 60 mA is measured in DCPD with 2 μm × 200 μm absorber and 60 μm delay length, which is 50% higher than the WIP device with the same waveguide dimension. To our best knowledge, this DCPD device also yields the highest power in the published WIP designs with similar absorbing area [5,7,8,11,12].

Figure 10 shows a failed DCPD, in which the overheated absorber region is 80 μm long in a device with a 200 μm long absorber. The overheated region is 12 μm long in the traditional waveguide structure photodiode fabricated on the same wafer, as shown in Fig. 2. This wider damaged region in DCPD shows that it not only distributes the absorption in a wider area, but also pushes the absorption peak further away from the front end.

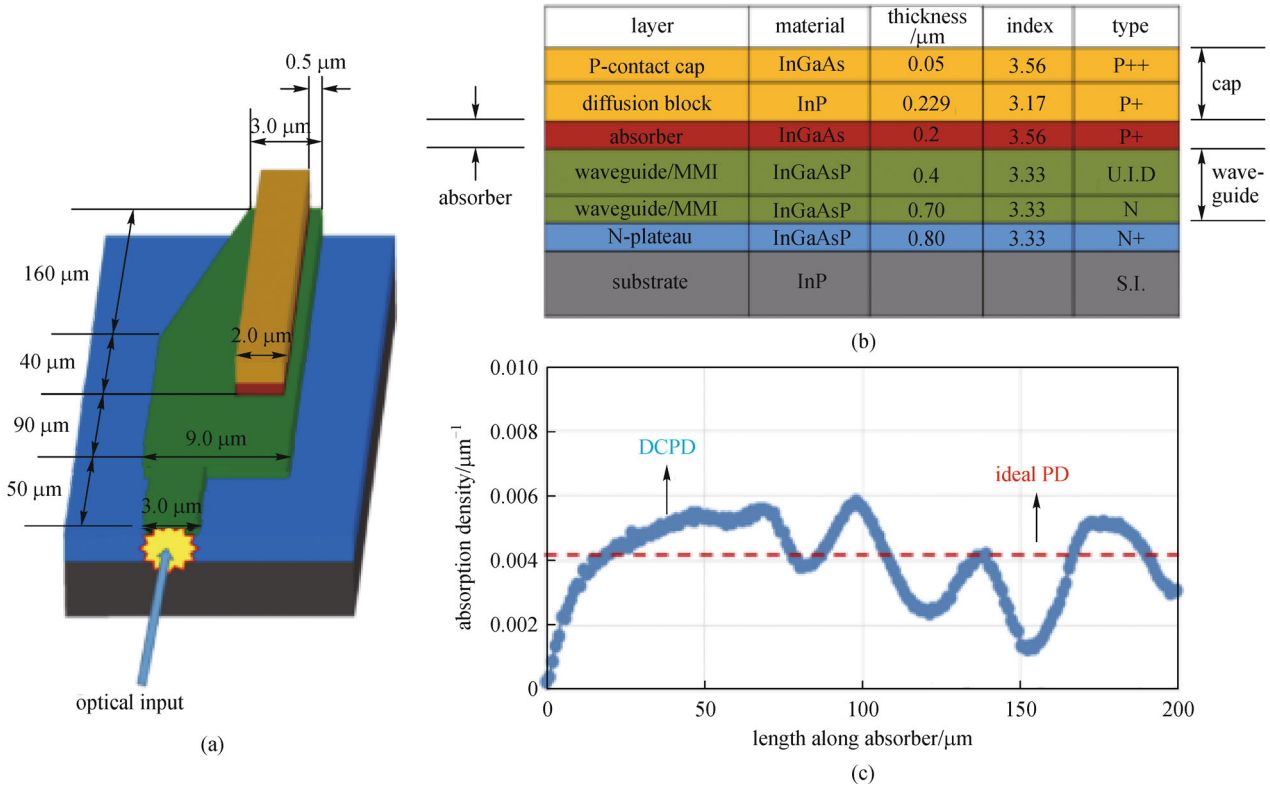

Fig. 8 Waveguide structure of DCPD (a); MUTC layer structure of DCPD (b); simulated absorption profile of DCPD (c)

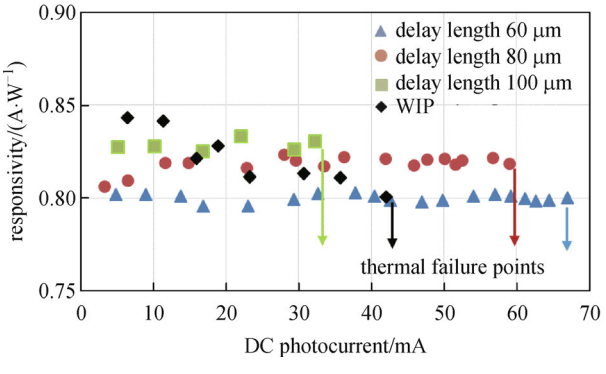

Fig. 9 DC optical power handling test of three DCPD devices with different delay lengths, in comparison with WIP device fabricated with the same waveguide dimension and the same layer structure with DCPD. The device responsivity is recorded at incremental photocurrent level until thermal failure happens

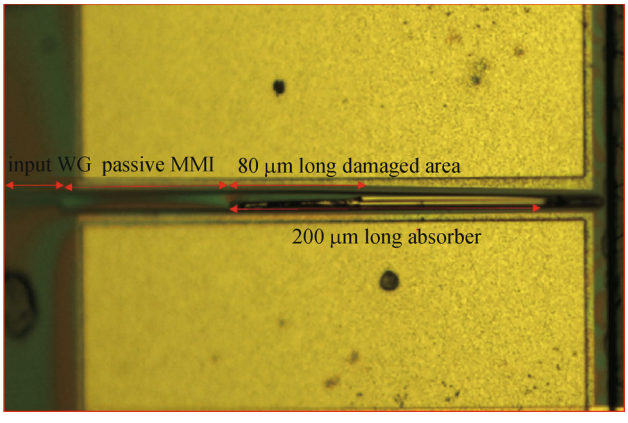

Fig. 10 Top view picture of thermally failed DCPD

4 DCPD for high bandwidth-efficiency product at high power

When operated under high power, DCPD design can outperform traditional WIP designs not only because it has better control of absorption near the front end, but also because it improves power handling capability without sacrificing bandwidth-efficiency product, which is essential for high speed performance. For high power applications, in the traditional WIP the reduction of absorption near the front end is achieved by reducing the confinement factor in the absorber. To achieve high absorption efficiency, it requires longer absorber length, which reduces the RC time limited bandwidth. In this case, conventional WIP's high power performance is typically accompanied by low bandwidth-efficiency product. In

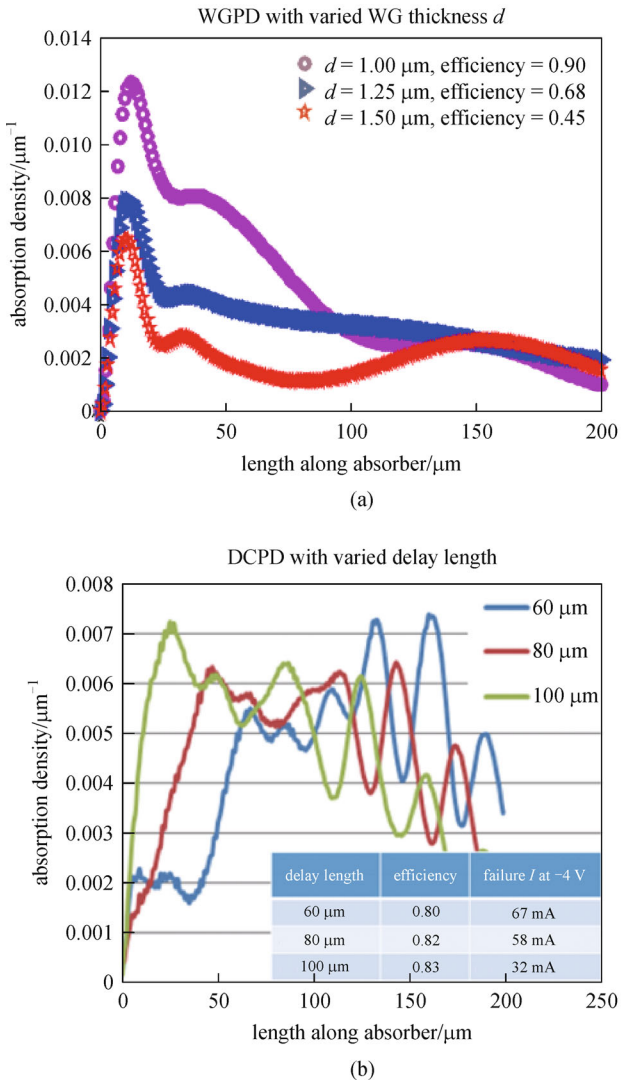

Fig. 11 Varying absorption near front end by changing WG thickness d in traditional WIP (a) and by changing delay length in DCPD (b)

contrast, the control of absorption near the front end of DCPD is decoupled from the absorption efficiency. It is mainly controlled by the delay length of the passive MMI section, while the absorption efficiency is mainly controlled by the power density in the MMI and the absorber length in the active section. For example, one can reduce the MMI width to increase the power density and improve the absorption efficiency; meanwhile, the delay length can be reduced to keep the absorption low near the front end. This distinct difference between traditional WIP and DCPD is demonstrated in Fig. 11, in which both the traditional WIP and DCPD waveguide structure are varied to reduce the absorption near the front end. In traditional WIP, the front end absorption can be reduced by increasing the waveguide thickness, but the absorption efficiency is reduced. In contrast, in DCPD the reduction of absorption near the front end is achieved by shortening the delay length, without affecting much the absorption efficiency. This is in good agreement with experimental results shown in Fig. 9, in which the improved power handling capability in DCPD with shorter delay length can be explained by the reduction of absorption near the front end as shown in the simulation.

5 Conclusions

Modal analysis of the traditional high power WIP design is presented, which points out the excitation of large Γ mode as the factor limiting the bandwidth-efficiency product at high power. We have theoretically and experimentally show that the DCPD waveguide can be designed to perform well under high power, and avoid the trade-off between bandwidth and absorption efficiency. Photocurrent > 60 mA under −4 V bias is measured in DCPD with 2 μm × 200 μm absorber area, which delivers the highest power in a similar absorber area among all WIP designs. Without affecting the bandwidth-efficiency product, the delay length can effectively control the absorption near front end in DCPD design. In this sense, DCPD represents a robust high power waveguide photodiode design for analog optical link.

Acknowledgements The author would like to acknowledge the funding support of ONR-MURI program (N00014-13-1-0678). The author would also like to thank Professor William S. C. Chang for many enlightening discussions on this subject.

References

1. Chang W S C. Fundamentals of Guided-Wave Optoelectronic Devices. Cambridge: Cambridge University Press, 2010
2. Williams K J, Esman R D, Dagenais M. Nonlinearities in pin microwave photodetectors. Journal of Lightwave Technology, 1996, 14(1): 84–96
3. Lasaosa D, Shi J W, Pasquariello D, Gan K G, Tien M C, Chang H H, Chu S W, Sun C K, Chiu Y J, Bowers J E. Traveling-wave photodetectors with high power-bandwidth and gain-bandwidth product performance. Quantum Electronics, 2004, 10(4): 728–741
4. Demiguel S, Giraudet L. Joulaud L, Decobert J, Blache F, Coupe V, Jorge F, Rossiaux P P, Boucherez E, Achouche M, Devaux F. Evanescently coupled photodiodes integrating a double-stage taper for 40-Gb/s applications-compared performance with side-illuminated photodiodes. Journal of Lightwave Technology, 2002, 20(12): 2004–2014
5. Michel N, Magnin V, Harari J, Marceaux A, Parillaud O, Decoster D, Vodjdani N. High-power evanescently-coupled waveguide photodiodes. IEE Proceedings-Optoelectronics, 2006, 153(4): 199–204
6. Jiang H, Yu P K L. High power waveguide integrated photodiode with distributed absorption. In: Proceedings of IEEE MTT-S Digest.

2000, 2: 679–682
7. Liao T S, Mages P, Yu P K L. Investigation of the high power integrated uni-traveling carrier and waveguide integrated photodiode. In: Proceedings of IEEE MTT-S Digest. 2003, 1: 155–158
8. Jiang H, Yu P K L. Waveguide integrated photodiode for analog fiber-optics links. IEEE Transactions on Microwave Theory and Techniques, 2000, 48(12): 2604–2610
9. Kato K, Yoshida J. Ultrawide-bandwidth 1.55 μm waveguide p-i-n photodiode. Proceedings of the Society for Photo-Instrumentation Engineers, 1994, 2149: 312–319
10. Draa M N, Bloch J, Chen D B, Scott D C, Chen N, Chen S B, Yu X C, Chang W S C, Yu P K L. Novel directional coupled waveguide photodiode-concept and preliminary results. Optics Express, 2010, 18(17): 17729–17735
11. Zhang Y X, Liao Z Y, Zhao L J, Zhu H L, Pan J Q, Wang W. A high-efficiency high-power evanescently coupled UTC-photodiode. Journal of Semiconductors, 2009, 30(4): 1–4
12. Klamkin J, Ramaswamy A, Johansson L A, Chou H F, Sysak M N, Raring J W, Parthasarathy N, DenBaars S P, Bowers J E, Coldren L A. High output saturation and high-linearity uni-traveling-carrier waveguide photodiodes. IEEE Photonics Technology Letters, 2007, 19(3): 149–151

Dingbo Chen is a graduate student in the Department of Electric and Computer Engineering, University of California at San Diego since 2008. He has been doing research on InP and Silicon based devices, including laser, modulator, and photodetector, which greatly enhance the performance of telecommunications network, His current focus on InGaAs waveguide photodiode with high power, high linearity, and high speed has the potential to push networking applications to next high level.

Rui Wang was born in Jilin Province, China. He obtained the Bachelor of Science degree in Department of Microelectronics, Peking University, Beijing, China, and the thesis Master of Applied Science degree on integrated optics in Department of Electrical and Computer Engineering, McMaster University, Canada. Currently he is pursing the Ph.D. degree on photonics in Department of Electrical and Computer Engineering, University of California, San Diego.